Proton-induced kinetic plasmon excitation in Al and Mg

S. M. Ritzau and R. A. Baragiola
University of Virginia, Laboratory for Atomic and Surface Physics, Thornton Hall, Charlottesville, Virginia 22901

R. C. Monreal
Universidad Autónoma de Madrid, Depto. Física Teórica de la Materia Condensada, C-V, Cantoblanco, 28049 Madrid, Spain

(Received 22 December 1998)

We report energy distributions of electrons emitted from Al and Mg surfaces bombarded by 3–100-keV/amu hydrogen and deuterium ions. The energy spectra contain structure consistent with the decay of bulk plasmons, even below the velocity threshold expected from current theories. To explain the results we compare the importance of additional mechanisms involving electron capture, lattice-assisted excitation, and excitation by fast secondary electrons. [S0163-1829(99)02423-6]

I. INTRODUCTION

One of the main ways in which fast charged particles lose energy in condensed matter is by exciting plasmons; collective excitation of valence electrons.[1] This mode of energy loss is especially important for materials of low atomic number Z, and for high-Z materials when the projectile velocity is insufficient to produce significant inner-shell excitations. In addition, the most common plasmon decay mechanism, a single-electron transition, can contribute to the emission of electrons from the solid.[2,3] Although plasmon excitation of metals by fast ions has attracted several theoretical studies,[3–6] experimental work for fast ion impact at energies of tens and hundreds of keV (Refs. 7–11) has been limited to identifying the plasmon decay structures seen in the electron emission spectra. In spite of the importance of plasmon excitation in energy loss and as source of electron emission for fast ions, quantitative studies of the plasmon excitation probabilities have only been done theoretically.

An electron-gas description of valence electrons leads to a minimum or threshold velocity $\nu_{\rm th}$ for plasmon excitations by a moving charge, determined by conservation of energy and momentum. This is shown with the aid of a diagram of allowed energy transfer $\hbar\omega$ vs momentum transfer $\hbar k$ in the excitation of a gas of free electrons (Fig. 1).[3] Allowed excitations by heavy particles occur at and below the straight lines $\hbar\omega = k\nu$, which, for projectile velocities $\nu < \nu_{\rm th}$ cannot intersect the plasmon line. For ions with mass much higher than the electron mass, the threshold velocity for exciting a narrow plasmon resonance is $\nu_{\rm th} \sim 1.3\nu_F$,[3] where ν_F is the Fermi velocity. A slightly lower threshold results from the small plasmon width in metals like Al and Mg. We note that excitation of plasmons by ions near $\nu_{\rm th}$ is not constrained by the available projectile energy, and this makes ions better suited than electrons for exploring the possible existence of excitations below the predicted threshold.

To study ion-induced plasmon excitations, we cannot use the projectile energy-loss method common in studies with fast electrons.[1,12] Characteristic energy losses are not observed with heavy projectiles because they are obscured by multiple energy losses from collisions with target nuclei. An alternative method to observe plasmons is through the electrons or photons that result from their decay.[12] Since the radiative channel is very unlikely, we have used electron spectroscopy for studying plasmon excitation. The characteristic spectral signature allows the separation of electrons from plasmon decay from those originating from other processes: Auger neutralization of the incoming ion at the surface,[13,14] direct ionizations in ion-atom and ion-electron collisions, and Auger decay of inner-shell excitations.[15] In the study we report here, we measured electron emission spectra from clean Al and Mg surfaces bombarded by H^+ and D^+ ions with incident velocities above and below $\nu_{\rm th}$ (3–100 keV/amu). We observed structure in the energy spectra of electrons even at velocities lower than $\nu_{\rm th}$. Below, we describe the experiments and discuss the discrepancy of the results with the theoretical expectation. Using simple models, we estimate theoretically the contributions of possible mechanisms giving rise to plasmon excitation, and compare these results with experiments.

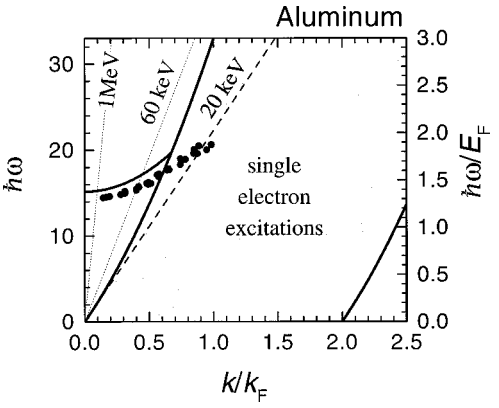

FIG. 1. The excitation spectrum of a free-electron gas with the density corresponding to Al, where $\hbar\omega$ and k are the energy and momentum transfer, respectively. The shaded area is the domain of single-particle excitations, and the line corresponds to the plasmon dispersion in the random-phase approximation. Maximum-energy-transfer lines for different proton energies are shown as straight lines. The points are from electron-energy-loss measurements of the plasmon resonance (Ref. 24).

II. EXPERIMENTS

The experiments were carried out in an ultrahigh-vacuum chamber (base pressure 8×10^{-10} Torr) using a spherical-sector electrostatic analyzer. The pass energy E_{pass} of the analyzer was set constant at 25 eV (resolution $\Delta E=0.2$ eV), and electrons were accelerated to E_{pass} by a programmable voltage applied to an entrance electrode. In this mode of operation, the transmission of the analyzer is approximately constant over the measured electron energy range. The analyzer work function ϕ_a was measured using 100-eV electrons following the procedure outlined in Ref. 16. For purposes of discussion, electron energies are shifted to refer to the vacuum level of the sample.

A focused, mass-analyzed ion beam from an ion accelerator entered the chamber from a differentially pumped chamber through a 1-mm-diameter aperture. The axis of the analyzer acceptance cone and the normal to the target surface were collinear, and the incidence angle of the ions was 60° with respect to this axis. Clean polycrystalline targets where obtained by vacuum depositing 40–100-nm-thick films from carefully outgassed Al and Mg (99.999% pure.) *In situ* Auger electron spectroscopy with 2.5–3-keV electrons showed the absence of contaminants above the detection limit of ~1%. To extend the projectile velocity range to lower values, we used deuterium ions, which are expected to be equivalent to protons of the same velocity, since isotope effects are negligible in electron emission at these velocities.[17] Incident electrons were also used to produce the plasmon decay structures, which were very similar to well-known electron-excited spectra reported previously.[18–20]

To accurately measure low-energy electrons, we used Helmholtz coils and a thin μ-metal liner to reduce the magnetic field in the region between the target and the analyzer to <2 mG, and biased the target to −5 V. The focusing effect on the detection efficiency, created by this bias and by the analyzer electro-optical elements, was checked by calculating electron trajectories.[21] The results were used to correct the collected spectra. We tested this correction by comparing spectra taken at different sample potentials.

III. RESULTS

Figures 2 and 3 show representative electron energy spectra $N(E)$ obtained from Mg and Al surfaces, respectively. The spectra are similar to spectra reported in the literature and obtained under different excitation conditions.[7,9,18–20] The spectra were normalized so their integral equals the total electron yields γ, which were measured by us and elsewhere.[22] A prominent shoulder is observed in the $N(E)$ spectra, similar to that seen for electron impact, which is due to the decay of bulk plasmons by excitation of a valence electron (interband transition) with simultaneous momentum exchange with the lattice. This process produces an electron energy distribution with a maximum energy of $E_m=E_b-\phi$, where E_b is the energy of the bulk plasmon, and ϕ is the work function of the target. The maximum energy E_m corresponds to the case where the plasmon is absorbed by an electron at the Fermi level. The high-energy edge of the shoulder is broadened by ~2 eV due to the finite plasmon lifetime.[23,24] Figures 2 and 3 also show derivative spectra dN/dE obtained using the Sawitsky-Golay algorithm, which introduces a broadening of ~0.5 eV. dN/dE has minima at E_m, from which we can determine the plasmon energy E_b.

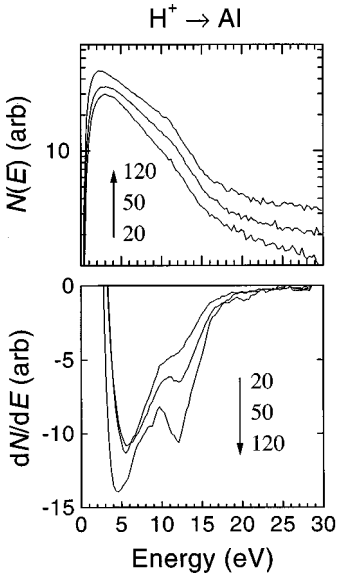

FIG. 2. Electron energy spectra $N(E)$ from Al bombarded by H^+ at 60° incidence. Bottom: derivative spectra $dN(E)/dE$. Parameter is the ion energy in keV.

The measured values of E_m are higher than $\hbar\omega_p$ $(k=0)$ expected for zero-momentum bulk plasmons (15.3 and 10.6 eV for Al and Mg respectively), and depend on projectile energy, as shown in Fig. 4. The shift in the plasmon energy with impact velocity is related to the plasmon dispersion, as shown in Fig. 1. In the region where pair excitations are allowed, the width of the plasmon resonance measured using electron energy loss is 3–5 times greater than those we see in the ion-induced secondary electron spectra.[24] Another significant finding is that, near v_{th}, the plasmon energy is observed to deviate significantly from the behavior expected from Fig. 1.

We do not see the surface plasmon clearly resolved from the peak in the energy distribution due to the surface barrier,

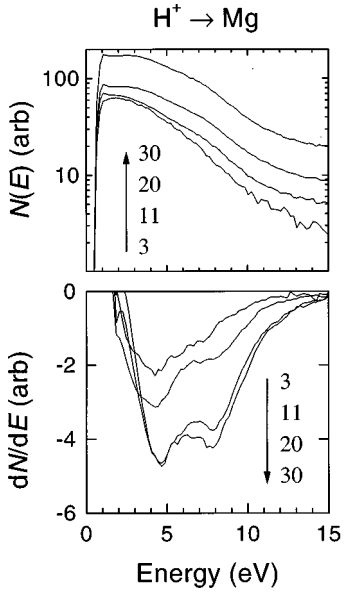

FIG. 3. Same as Fig. 2, but for Mg.

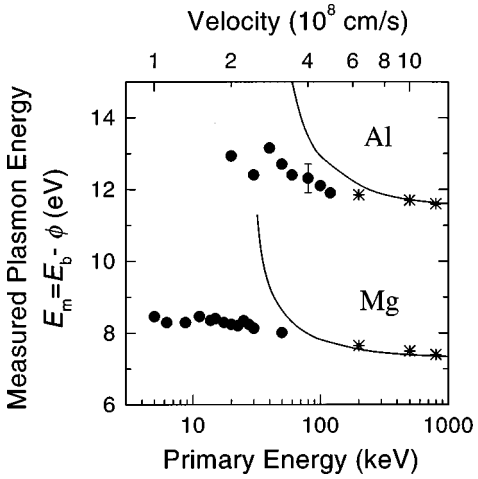

FIG. 4. Plasmon energies derived from the plasmon high-energy edge, measured in the derivative spectra, vs projectile velocity. Also shown are data from Ref. 9 (*) and the RPA predictions (solid lines).

as seen in the spectrum of Hasselkamp and Scharmann for 500-keV H^+ impact on Al at normal incidence.[9] We attribute this to the fact that excitation should be low due to our use of lower velocities and oblique (60°) incidence.[25] The spectra of Benazeth *et al.*,[15] measured for 60-keV H^+ at 60° incidence, also lack this feature. For Mg targets, structure due to surface plasmon decay occurs at ~3.5 eV and so it cannot be separated with certainty from the low-energy peak in $N(E)$ created by the surface barrier.

To quantify the number of electrons emitted due to bulk-plasmon decay, we must distinguish them from those due to all other processes. The method we used is illustrated graphically in Fig. 5. The high-energy continuum tail above $E_m + \Delta E_m$ is well represented by a function of the form $N_t(E) = BE^n$, where B and n are constant fitting parameters. We slightly extrapolate $N_t(E)$ to E_m to obtain the number of electrons from plasmon decay, at E_m, as $N_p(E_m) = N(E_m) - N_t(E_m)$. Subtraction of a power-law background was used and justified by Sickafus[26] to separate sources of secondary electrons from the continuum background. To reduce the error associated with the choice of the exact value of E_m, we

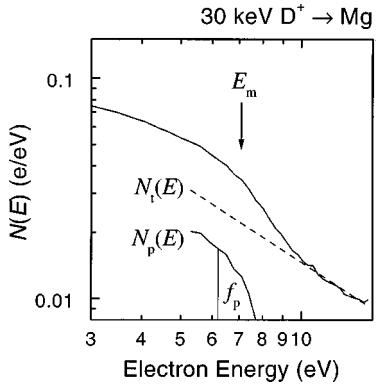

FIG. 5. The extraction of the fractional plasmon decay yield, f_p, from a measured spectrum, showing the extrapolated high-energy tail $N_t(E)$ which we subtract from the measured $N(E)$ to obtain $N_p(E)$. E_m is the position of the local minimum of $dN(E)/dE$.

integrate $N_p(E) = N(E) - N_t(E)$ over a small energy region $2\delta = 2$ eV corresponding to the plasmon full width at half maximum, and calculate the fraction of emitted electrons which are due to plasmon decay,

$$f_p = \frac{\gamma_p}{\gamma} = \frac{C(v_0)}{\gamma} \int_{E_m - \delta}^{E_M + \delta} N_p(E) dE, \tag{1}$$

where γ_p is the electron yield due to plasmon decay, and the factor $C(v_0)$ relates the integral of $N_p(E)$ about E_m over the range 2δ to the integral of $N_p(E)$ over all E. Although we do not know the exact form of $N_p(E)$ outside of the region near E_m, we can estimate $N_p(E)$ to obtain an approximate result. We approximate $N_p(E)$ using a parabolic density of states uniformly shifted by E_m, and then convoluted with a 2-eV-wide Gaussian to account for the plasmon width. We estimate $C = 8$ (Al) and 5 (Mg). Because the broadening in the distribution of secondary electrons is symmetric about E_m, and the integration width we use always exceeds the plasmon width, C is independent of primary velocity. Our estimated values of C for H+ on Al are consistent with the values obtained from plasmon decay spectra calculated by Rösler,[27] divided by cos60° to account for oblique incidence. He found that, for Al (Mg), $C(\nu_0)$ ranges from 5 to 12 (5 to 3) for energies from 100 to 1000 keV. Other methods of background subtraction applied to the data, including modeling the secondary distributions using the theory of Schou[28] and use of the derivative spectra, were found to produce results with greater uncertainties.

Since f_p is determined using $N_p(E)$, and the exact shape of $N_p(E)$ is not known, the uncertainty in f_p was obtained by varying the plasmon energy, integral width δ, background level, and value of $C(\nu_0)$, and determining their effect of the value of f_p for representative spectra. For a shift in the plasmon energy E_m of $\pm\Delta E = 0.7$ eV (the sum of the analyzer resolution and the broadening due to the numerical derivative algorithm), we found $(\delta f_p / f_p)_E \sim 0.05$. A variation of the integral width of $0.3 < \delta < 1.5$ eV produced $(\delta f_p / f_p)_\delta \sim 0.07$. We assign generous errors of 20% in the background level evaluated at E_m, and an additional 20% uncertainty in $C(\nu_0)$. Adding all errors in quadrature gives uncertainties $(\Delta f_p / f_p) \sim 0.3$ and $(\Delta \gamma_p / \gamma_p) \sim 0.32$.

Figures 6 and 7 show γ_p as a function of projectile energy for Al and Mg, respectively. In them, one can see substantial plasmon excitation below the predicted threshold $\nu_{\rm th}$ for both Al and Mg. The results for Al are compared to the theory by Rösler[3] above $\nu_{\rm th}$. The ratio γ_p / γ is consistent with the value for 500-keV H^+ we extract from the data of Ref. 9 using the same procedure described above.

IV. DISCUSSION

If the observed plasmon excitation below $\nu_{\rm th}$ results directly from interactions with the projectile, our findings would imply the need to revise existing theories of plasmon excitation and electronic energy loss at low velocities. On the other hand, plasmons may be produced by secondary processes involving fast electrons resulting from single-particle excitations. We explore several mechanisms that may explain the observations. The first is the relaxation of the energy-momentum conservation criteria for an electron

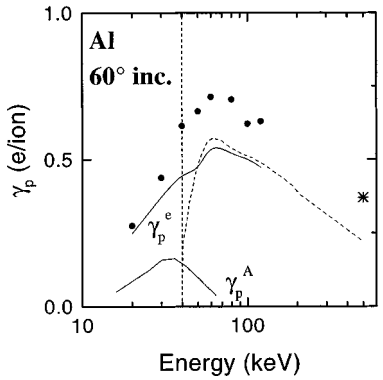

FIG. 6. Electron yield due to plasmon decay, γ_p (electrons/ion), as a function of incident energy for proton impact on Al. Also shown are the theoretical predictions of Rösler (Ref. 3), adjusted for oblique incidence (dashed line), the plasmon-assisted electron capture yield γ_p^A given by Eq. (5), and the electron yield due to plasmons excited by energetic secondary electrons γ_p^e from Eq. (12). Also shown are data from Ref. 9 (*).

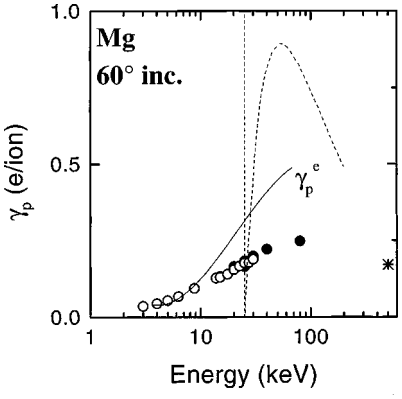

FIG. 7. Same as Fig. 6, but for Mg. ●, H^+; ○, D^+.

gas, possible if the lattice absorbs momentum during the excitation event by an umklapp process. This mechanism is unlikely, as judged from the very weak plasmon excitation by photons in interactions with valence electrons,[29] which require a similar absorption of momentum by the lattice. The fact that plasmon energies do not deviate much from the $k=0$ value suggests that this process is also not very important. Reinforcing the argument is the fact that the calculations of the electronic energy loss of protons in Al crystal (i.e., lattice included) and in Al jellium[30] differ by only 10% differences for proton velocities smaller than 2×10^8 cm/s.

Plasmon excitations that accompany the neutralization near surfaces of slow ions ($v \ll v_F$) with high potential energy (potential excitation) have been recently observed for noble-gas ions on Al and Mg,[31] and multiply-charged ions on Al.[32] This type of excitation was first predicted by Lucas and Šunjic,[33] and described theoretically[34–37] for the case of surface plasmons. For Al and Mg, bulk-plasmon excitation cannot occur for stationary protons because the potential energy available for excitation $E_n = IP' - \phi$ is insufficient[31] (IP' is the ionization potential of H minus a ~2-eV image shift). The situation changes for moving protons. Here the energy distribution of valence electrons is shifted in the frame of the ion, increasing the maximum energy release accompanying neutralization, by $\sim m v v_{\text{Fermi}}$.

Plasmon excitation by electron capture can also occur in the bulk of the solid, both for protons ($H^+ \rightarrow H$) and for H resulting from electron capture collisions in the solid ($H \rightarrow H^-$). The probability that a plasmon is excited between times t and $t+dt$ is[38]

$$P(t) = \Phi^+(t)\frac{dt}{\tau^+} + \Phi^0(t)\frac{dt}{\tau^0}, \tag{2}$$

where $\Phi^+(t)$ [$\Phi^0(t)$] is the fraction of H^+(H) existing at time t in the solid, and dt/τ^+ (dt/τ^0) is the probability that H^+(H) captures an electron with excitation of a plasmon. We are interested in the spectrum of the electrons emitted by the decay of this plasmon. In Eq. (34.1) of Ref. 32 we find that either of the transition rates $1/\tau^+$ or $1/\tau^0$ can be calculated as

$$\frac{1}{\tau^{+,0}} = \int_{\omega_p}^{\omega_c} d\omega \frac{dP^{+,0}}{d\omega}.$$

Then $dP^+/d\omega$ gives us the rate at which plasmons of energy $\hbar\omega$ in an energy range $\hbar\, d\omega$ are excited in the Auger capture process. We assume that all plasmons decay by imparting their energy to a single electron. The probability that a plasmon of energy $\hbar\omega$ produces an electron above the Fermi level at an energy ε_p, in an interval $d\varepsilon_p$, is written as

$$\frac{dP_{\text{decay}}(\varepsilon_p,\omega)}{d\varepsilon_p} = \frac{\rho(\varepsilon_p)\rho(\varepsilon_p-\hbar\omega)\Theta(\varepsilon_p-E_F)\Theta(E_F-\varepsilon_p+\hbar\omega)}{\int d\varepsilon'\rho(\varepsilon')\rho(\varepsilon'+\hbar\omega)\Theta(\varepsilon'+\hbar\omega-E_F)\Theta(E_F-\varepsilon')}, \tag{3}$$

where $\rho(\varepsilon)$ is the free-electron density of states, E_F the Fermi energy, and Θ the step function. We also assume that the plasmon produced at a depth z decays at the same depth. We consider that the probability that one electron is collected outside the surface is given by $1/2Te^{-z/L}$, where z is the depth in the solid. The factor $\frac{1}{2}$ takes into account that, on the average, only half of the electrons travel toward the surface. $T(\varepsilon) = (\varepsilon - W)/\varepsilon$ is the probability that an electron with energy ε is transmitted through the surface barrier of height W, and $L(\varepsilon)$ is the calculated inelastic mean free path.[38] The expression for T follows the assumption that the electron motion inside the solid is made isotropic by strong elastic scattering at these low energies.[39] Finally, the spectrum of electrons produced by the decay of plasmons excited in the Auger capture processes is calculated as the product of all probabilities integrated over the incoming path of the ion $z = vt/\cos(\theta)$

$$\frac{d\gamma_p^A(\varepsilon_p)}{d\varepsilon_p} = \frac{\cos(\theta)}{\nu}\int dz\,\frac{T(\varepsilon_p)}{2}e^{-z/L} \times \int d\omega\,\frac{dP_{\rm decay}(\varepsilon_p,\omega)}{d\varepsilon_p} \times\left(\Phi^+\frac{dP^+}{d\omega}+\Phi^0\frac{dP^0}{d\omega}\right), \tag{4}$$

where ν is the ion velocity, and θ the incidence angle with respect to the surface normal. Φ^+ and Φ^0 have two contributions due to charge ''equilibrium'' at large depth, and from the initial conditions at $t=0$. As a further approximation we only consider the contribution of $\Phi^{+\rm eq}$ and $\Phi^{0\rm eq}$ which we take from Ref. 38, and obtain the yield of electrons from this capture processes as

$$\gamma_p^A = \int d\varepsilon_p \frac{d\gamma_p^A}{d\varepsilon_p}, \tag{5}$$

where the integration is performed on an energy window ± 1 eV, like in the experiment. The result of Eq. (5) for Al is plotted in Fig. 6. The bell shape of the curve is the consequence of the opposite behaviors of $\Phi^{+\rm eq}$ and $1/\nu\tau^+$ with projectile velocity; when ν increases, the H^+ fraction increases and the capture probability per unit path length decreases. We find that the second term on the right-hand side of Eq. (2) only contributes appreciably to the plasmon intensity for projectile energies less than 16 keV/amu; above this value, the first term dominates. It can be seen from Fig. 6 that plasmon excitation by electron capture is not the dominant factor determining the existence of plasmon excitation below $\nu_{\rm th}$.

Finally, we consider plasmon excitation by fast secondary electrons produced by the projectile. One source of energetic electrons is the Auger decay of L-shell vacancies in target atoms, excited by the incoming projectile. The cross section for production of LVV Auger electrons by protons at velocities just below $\nu_{\rm th}$ is $\sigma_A \sim 4\times 10^{-18}$ cm^2/atom for Mg,[15] corresponding to a mean free path between excitations of 425 Å. Thus the excitation probability is only 0.02 over the 9-Å mean escape depth[39] of 10-eV electrons (representing plasmon decay). The value is even lower for Al, where the cross section for L-shell excitation near $\nu_{\rm th}$ is about a factor of 4 smaller.[15] Therefore, the very small excitation probability of inner shells strongly discounts Auger electrons as a significant mechanism for plasmon excitation below $\nu_{\rm th}$.

A more abundant source of energetic electrons is the binary proton-electron interactions in the solid. To calculate the electron yield due to the decay of electron-excited plasmons γ_p^e, we consider a proton moving with velocity $\nu_{\rm in}$ in the solid near the surface, exciting electrons of energy ε_e with probability $P_{\rm in}(\nu_{\rm in}\varepsilon_e)$. $P_{\rm in}$ is taken to be independent of depth z since protons suffer negligible angular scattering and energy loss over the electron escape depth (a few nm) at these incident velocities.[39] We again assume that the electron motion inside the solid is made isotropic by strong elastic scattering at these low energies, so that the electron has an equal probability of traveling toward or away from the surface.

Our treatment of the electrons will be slightly different for these two directions. We first consider a fast electron headed toward the surface. After traveling some distance, it may excite a plasmon at a depth z' with a probability P_1 given by the product of the probability that it does not suffer a collision on its way to z', and the probability that it will produce a plasmon at z':

$$P_1 = \exp\left(-\frac{(z-z')}{L}\right)\frac{dz'}{l_p}, \tag{6}$$

where $l_p(\varepsilon_e)$ is the mean free path to excite a plasmon, and $L(\varepsilon_e)$ is the total inelastic mean free path. Equation (6) assumes that plasmons can only be excited in the first collision event; this is because an electron loses a large fraction of its energy in one collision, and thus it is unable to excite a plasmon in a second one. Thus an energy-loss event, either by exciting a plasmon or another electron, is sufficient to remove the electron from the high-energy tail, and should be a good approximation at the energies of interest, <40 eV for Al. To determine l_p, we use the random-phase-approximation (RPA) expression[38]

$$\frac{1}{l_p} = \frac{1}{\nu_e}\int_{\omega_p}^{\omega_c} d\omega\,\frac{dP(\varepsilon_e,\omega)}{d\omega}, \tag{7}$$

where ν_e is the electron velocity, ω_p and ω_c are the plasmon frequencies at $k=0$ and at the cut-off momentum k_c, respectively, and $dP(\varepsilon_e,\omega)/d\omega$ is the rate at which an electron of energy ε_e will produce a plasmon of energy $\hbar\omega$.

We assume that the plasmon produced at z' decays at z' as well, producing an electron with energy ε. The probability that a secondary electron of energy ε_e produces a plasmon of energy $\hbar\omega$ that decays into an electron of energy ε is then given by the product

$$P_2 = \frac{dP(\varepsilon_e,\omega)}{d\omega}\times\frac{dP_{\rm decay}(\varepsilon,\omega)}{d\varepsilon}, \tag{8}$$

where the second term is given by Eq. (3). Again, the (plasmon-decay) electron has an equal probability of traveling toward the surface or away from it. Considering only those electrons which are heading to the surface, we apply an attenuation factor of $\exp[-z'/L(\varepsilon)]$ to account for transport to the surface. We combine the results of Eqs. (6)–(8) and integrate over z, z', ω, and ε_e to obtain the number of electrons of energy ε.

$$\left(\frac{d\gamma_p^e}{d\varepsilon}\right)_{\rm out} = \int d\varepsilon_e\int_0^\infty \frac{dz}{\cos(\theta)}P_{\rm in}(\nu_{\rm in},\varepsilon_e)\int_0^z dz'\,\frac{1}{2}\exp\left(-\frac{z-z'}{L(\varepsilon_e)}\right)\frac{1}{2}\exp\left(-\frac{z'}{L(\varepsilon)}\right) \times T(\varepsilon)\,\frac{1}{\nu_e}\int_{\omega_p}^{\omega_c} d\omega\,\frac{dP(\varepsilon_e,\omega)}{d\omega}\frac{dP_{\rm decay}(\varepsilon,\omega)}{d\varepsilon}. \tag{9}$$

To determine $P_{\rm in}(\nu_{\rm in},\varepsilon_e)$ we use the measured tail of $N(E)$ at energies higher than the minimum value to excite plasmons, which is ~18.7 (12.1) eV above the vacuum level for Al (Mg) in the RPA. This tail has the form $N_t(E)=B/E^p$, with $\varepsilon_e=E+W$. This gives

$$P_{\rm in}(\nu_{\rm in},\varepsilon_e)=\frac{2B\cos(\theta)}{L(\varepsilon_e)E^pT(\varepsilon_e)}. \tag{10}$$

Substituting Eq. (10) into Eq. (9) and integrating in z and z', we find

$$\left(\frac{d\gamma_p^e}{d\varepsilon}\right)_{\rm out}=\int d\varepsilon_e\frac{B}{E_p}\frac{1}{2}\frac{T(\varepsilon)}{T(\varepsilon_e)}\frac{L(\varepsilon)}{\nu_e}\int_{\omega_p}^{\omega_c}d\omega\frac{dP(\varepsilon_e,\omega)}{d\omega}\times\frac{dP_{\rm decay}(\varepsilon,\omega)}{d\varepsilon}. \tag{11}$$

While we ignore the plasmon-decay electrons that are headed into the solid, we must now consider the fast secondary electrons that were headed in that direction. The development for these electrons is exactly the same as for the proton-excited electrons which were headed out of the solid, using the corresponding exponential factor in Eq. (6). We combine these electrons with those in Eq. (11) to obtain the energy distribution of electrons due to plasmon decay:

$$\frac{d\gamma_p^e}{d\varepsilon}=\int d\varepsilon_e\frac{B}{E^p}\frac{T(\varepsilon)}{T(\varepsilon_e)}\left(\frac{1+L(\varepsilon_e)/2L(\varepsilon)}{1+L(\varepsilon_e)/L(\varepsilon)}\right)\frac{L(\varepsilon)}{\nu_e}\times\int_{\omega_p}^{\omega_c}d\omega\frac{dP(\varepsilon_e,\omega)}{d\omega}\times\frac{dP_{\rm decay}(\varepsilon,\omega)}{d\varepsilon}. \tag{12}$$

Using linear-response theory, we find $dP(\varepsilon_e,\omega)/d\omega$, the rate at which a particle excites plasmons of energy ω. It is given essentially by Eq. (6.1) of Ref. 38 integrated in q and with $\mathrm{Im}[-1/\varepsilon(q,\omega)]$ evaluated only on the plasmon line. Numerical integration over ε gives γ_p^e. Because we obtain $d\gamma_p^e/d\varepsilon$, which is a calculation of $N_p(E)$, we can also determine values of $C(v_0)$ for Al and Mg. We find $C(\nu_0)$ range from 6.75 to 7.1 over the energy range of interest for Al, and from 3.9 to 4.9 for Mg.

Calculated values of $d\gamma_p^e$ are shown in Figs. 6 and 7 for Al and Mg, respectively. For Al, the agreement with experiment at low ν suggests that energetic secondary electrons are an important source of plasmons, and can explain the discrepancy between theory and experiment below $\nu_{\rm th}$. For Mg, we also obtain good agreement at the lower velocities, but the model overestimates the yields at velocities above the threshold for direct plasmon excitation. A plausible source for this discrepancy is that we have not considered that due to the *begrenzung* effect,[25,40] near the surface part of the excitation of plasmons that we calculate actually results in surface plasmons, which we do not measure. This effect is more important in Mg and at high proton velocities where the mean free path of the electrons is smaller due to a larger relative contribution of high-energy electrons. We note that there are other uncertainties in the model, like the localization of the plasmon decay, and the simplified treatment of electron transport. Nevertheless, the fact that theory and experiment are close at low velocities, where the contribution of the higher-energy electrons is smaller, suggest that energetic secondary electrons are the main source of plasmon excitations at velocities lower than $\nu_{\rm th}$. The importance of secondary electrons in producing relatively high-energy excitations in metals parallels that found in the efficient ionization of dense gases or insulators. In condensed Ar (band gap 14.2 eV), half the ionizations are produced by secondary electrons for 100-keV incident protons.[2]

The mechanism of plasmon excitation due to fast electrons should also need a velocity above a threshold value. This results because the maximum energy transfer from a proton to an electron at the Fermi level, $2m\nu(\nu-\nu_{\rm Fermi})$ (Ref. 17), must lead to a final electron energy exceeding the minimum energy for plasmon excitation. The value of this threshold $\nu'_{\rm th}$ is $0.74(0.64)\times10^8$ cm/s for Al (Mg), lower than $\nu_{\rm th}$ and than the smallest velocities used in this study. These thresholds correspond to 2.9 and 2.1 keV/amu for Al and Mg, respectively.

We note that in Figs. 6 and 7 the experiments do not show a discontinuity at the threshold for direct plasmon excitation, as predicted by Rösler's theory.[3] Possible reasons for this are the neglect of projectile neutralization and the limitations of the free-electron RPA. The effect of projectile neutralization would be a decrease in the plasmon yield that is more pronounced at the lowest velocities, thus smoothing the onset at the threshold. However, RPA theories of electronic energy loss that take charge exchange into account also give a discontinuity at $\nu_{\rm th}$ (e.g., Ref. 41). Thus we are led to the conclusion that the abrupt threshold for direct plasmon excitation is a characteristic of this type of free-electron approximation.

In conclusion, we have observed that plasmon excitation and decay in collisions of 5–100-keV protons with Mg and Al metals is an important electron emission mechanism. The energy dependence of plasmon excitation agrees with the theory of Rösler[3] at higher energies, but we observe significant plasmon excitation at velocities below the threshold predicted by theory (40 and 25 keV/amu for Al and Mg, respectively). We analyze several causes for the discrepancy, and conclude that the most plausible one is plasmon excitation by fast secondary electrons resulting from binary ion-electron collisions. This result has several implications: (i) Since the maximum electron energy depends on the projectile velocity, there is a threshold velocity for this secondary plasmon excitation that is substantially lower than that for direct excitation. (ii) Plasmon excitation by secondary electrons will be particularly important when using highly charged projectiles, since they are important sources of energetic Auger electrons. (iii) There appears to be a significant discrepancy with current theories of energy loss regarding the onset of the contribution of direct plasmon excitations.

ACKNOWLEDGMENTS

We thank M. Rösler, S. Schnatterly, and J. García de Abajo for useful discussions. This work was supported by the National Science Foundation, Division of Materials Research, the Southwest Research Institute, Iberdrola S.A., and the Spanish Comisión Interministerial de Ciencia y Tecnología, Contract No. PB97-0044.

[1] H. Raether, *Excitation of Plasmons and Interband Transitions by Electrons* (Springer-Verlag, Berlin, 1980).
[2] R. A. Baragiola, Nucl. Instrum. Methods Phys. Res. B **78**, 223 (1993).
[3] M. Rösler, Scanning Microsc. **8**, 3 (1994); Appl. Phys. A: Mater. Sci. Process. **61**, 595 (1995); Nucl. Instrum. Methods Phys. Res. B **115**, 278 (1996); in *Ionization of Solids by Heavy Particles*, edited by R. A. Baragiola (Plenum, New York, 1990), p. 27.
[4] R. Zimmy, Surf. Sci. **260**, 347 (1992).
[5] F. J. García de Abajo and P. M. Echenique, Nucl. Instrum. Methods Phys. Res. B **79**, 15 (1993); F. J. García de Abajo, *ibid.* **98**, 445 (1995).
[6] J. A. Gaspar, A. G. Eguiluz, and D. L. Mills, Phys. Rev. B **51**, 14604 (1995).
[7] N. M. Omel'yanovskaya and S. Ya. Lebedev, Fiz. Tverd. Tela (Leningard) **15**, 2778 (1973) [Sov. Phys. Solid State **15**, 1848 (1973)].
[8] C. Benazeth, N. Benazeth, and L. Viel, Surf. Sci. **78**, 625 (1978).
[9] D. Hasselkamp and A. Scharmann, Surf. Sci. **119**, L388 (1982); S. Hippler, Ph.D. thesis, University of Giessen, Germany, 1988.
[10] M. F. Burkhard, H. Rothard, and K.-O. E. Groeneveld, Phys. Status Solidi B **147**, 589 (1988).
[11] N. J. Zheng and C. Rau, J. Vac. Sci. Technol. A **11**, 2095 (1993).
[12] A. Liebsch, *Electronic Excitations at Metal Surfaces* (Plenum, New York, 1997).
[13] H. D. Hagstrum, Phys. Rev. **96**, 336 (1954); and in *Chemistry and Physics of Solid Surfaces VII*, edited by R. Vanselow and R. F. Howe (Springer-Verlag, Berlin, 1988), p. 341.
[14] R. A. Baragiola, Radiat. Eff. **61**, 47 (1982); R. A. Baragiola, in *Low Energy Ion-Surface Interactions*, edited by J. W. Rabalais (Wiley, New York, 1994), Chap. 4.
[15] C. Benazeth, N. Benazeth, and L. Viel, Surf. Sci. **78**, 625 (1978); C. Benazeth, M. Hou, N. Benazeth, and C. Mayoral, Nucl. Instrum. Methods Phys. Res. B **33**, 295 (1988).
[16] R. A. Baragiola, in *Low Energy Ion-Surface Collisions* (Academic, New York, 1977), p. 283.
[17] R. A. Baragiola, E. V. Alonso, and A. Oliva-Florio, Phys. Rev. B **19**, 121 (1979).
[18] N. B. Gornyi, Fiz. Tverd Tela (Leningard) **8**, 1939 (1966) [Sov. Phys. Solid State **8**, 1535 (1966)]; Zh. Eksp. Teor. Fiz. **37**, 23 (1960) [Sov. Phys. JETP **10**, 15 (1960)].
[19] L. H. Jenkins and M. F. Chung, Surf. Sci. **33**, 159 (1972).
[20] M. S. Chung and T. E. Everhart, Phys. Rev. B **15**, 4699 (1977).
[21] Simion 6.0 3D electrostatic analysis program, Idaho National Eng. Lab. Idaho Falls, ID.
[22] E. V. Alonso, R. A. Baragiola, and A. Oliva-Florio (unpublished).
[23] T. Kloos, Z. Phys. **265**, 225 (1973).
[24] P. C. Gibbons, S. E. Schnatterly, J. J. Ritsko, and J. R. Fields, Phys. Rev. B **13**, 2451 (1976).
[25] C. Denton, J. L. Gervasoni, R. O. Barrachina, and N. R. Arista, Phys. Rev. A **37**, 4498 (1998).
[26] E. N. Sickafus, Phys. Rev. B **16**, 1436 (1977).
[27] M. Rösler (private communication).
[28] J. Schou, Phys. Rev. B **22**, 2141 (1980).
[29] S. A. Flodström, L.-G. Petersson, and S. B. M. Hagström, Solid State Commun. **19**, 257 (1976).
[30] I. Campillo, J. M. Pitarke, and A. G. Eguiluz, Phys. Rev. B **58**, 10 307 (1998).
[31] R. A. Baragiola and C. A. Dukes, Phys. Rev. Lett. **76**, 2547 (1996).
[32] D. Niemann, M. Grether, M. Rösler, and N. Stolterfoht, Phys. Rev. Lett. **80**, 3328 (1998).
[33] A. A. Lucas and M. Šunjic, Surf. Sci. **32**, 439 (1972).
[34] A. A. Almuellen and M. D. Girardeau, Surf. Sci. **210**, 138 (1989).
[35] F. A. Gutierrez, Surf. Sci. **370**, 77 (1997).
[36] R. Monreal and N. Lorente, Phys. Rev. B **52**, 4760 (1995); R. Monreal, Surf. Sci. **388**, 231 (1997).
[37] M. A. Vicente Alvarez, V. H. Ponce, and E. C. Goldberg, Phys. Rev. B **57**, 14 919 (1998).
[38] P. M. Echenique, F. Flores, and R. H. Ritchie, in *Solid State Physics: Advances in Research and Applications*, edited by H. Ehrenreich and D. Turnbull (Academic, New York, 1990), Vol. 43, p. 229.
[39] C. J. Tung and R. H. Ritchie, Phys. Rev. B **16**, 4302 (1977).
[40] S. M. Bose, S. Prutzer, and P. Longe, Phys. Rev. B **27**, 5992 (1983).
[41] M. Peñalba, A. Arnau, P. M. Echenique, F. Flores, and R. H. Ritchie, Europhys. Lett. **19**, 45 (1992).